Title
Proton Exchange Membrane Fuel Cell Characterization for Electric Vehicle Applications

Authors
Swan, D.H.
Dickinson, B.E.
Arikara, M.P.

Publication Date
1994-02-01

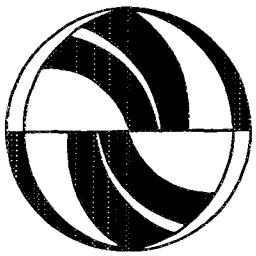

Proton Exchange Membrane Fuel Cell Characterization for Electric Vehicle Applications

D.H. Swan
B.E. Dickinson
M.P. Arikara

Reprint
UCTC No. 257

The University of California
Transportation Center

University of California
Berkeley, CA 94720

The University of California Transportation Center

The University of California Transportation Center (UCTC) is one of ten regional units mandated by Congress and established in Fall 1988 to support research, education, and training in surface transportation. The UC Center serves federal Region IX and is supported by matching grants from the U.S. Department of Transportation, the California Department of Transportation (Caltrans), and the University.

Based on the Berkeley Campus, UCTC draws upon existing capabilities and resources of the Institutes of Transportation Studies at Berkeley, Davis, Irvine, and Los Angeles; the Institute of Urban and Regional Development at Berkeley; and several academic departments at the Berkeley, Davis, Irvine, and Los Angeles campuses. Faculty and students on other University of California campuses may participate in Center activities. Researchers at other universities within the region also have opportunities to collaborate with UC faculty on selected studies.

UCTC's educational and research programs are focused on strategic planning for improving metropolitan accessibility, with emphasis on the special conditions in Region IX. Particular attention is directed to strategies for using transportation as an instrument of economic development, while also accommodating to the region's persistent expansion and while maintaining and enhancing the quality of life there.

The Center distributes reports on its research in working papers, monographs, and in reprints of published articles. It also publishes *Access*, a magazine presenting summaries of selected studies. For a list of publications in print, write to the address below.

University of California Transportation Center

108 Naval Architecture Building
Berkeley, California 94720
Tel: 510/643-7378
FAX: 510/643-5456

Proton Exchange Membrane Fuel Cell Characterization for Electric Vehicle Applications

D.H. Swan
B.E. Dickinson
M.P. Arikara

Institute of Transportation Studies
University of California at Davis
Davis, CA 95616

Reprinted from
Advancements in Electric and Hybrid Electric Vehicle Technology
Society of Automotive Engineers, SP-1023, February 1994

UCTC No. 257

The University of California Transportation Center
University of California at Berkeley

940296

Proton Exchange Membrane Fuel Cell Characterization for Electric Vehicle Applications

D. H. Swan, B. E. Dickinson, and M. P. Arikara
University of California, Davis

ABSTRACT

This paper presents experimental data and an analysis of a proton exchange membrane fuel cell system for electric vehicle applications. The dependence of the fuel cell system's performance on air stoichiometry, operating temperature, and reactant gas pressure was assessed in terms of the fuel cell's polarity and power density-efficiency graphs. All the experiments were performed by loading the fuel cell with resistive heater coils which could be controlled to provide a constant current or constant power load. System parasitic power requirements and individual cell voltage distribution were also determined as a function of the electrical load. It was found that the fuel cell's performance improved with increases in temperature, pressure and stoichiometry within the range in which the fuel cell was operational. Cell voltage imbalances increased with increases in current output. The effect of such an imbalance is, however, not detrimental to the fuel cell system, as it is in the case of a battery.

INTRODUCTION

An electrochemical fuel cell is a device that converts chemical energy to direct current electrical energy. By converting an on-board fuel to electricity it could be effectively used to power an electric vehicle. As such, a fuel cell is an energy conversion device like an internal combustion engine. This is in contrast to energy storage systems such as batteries, flywheels and ultra capacitors. Further many of a fuel cells operating characteristics are closer to that of an engine than a storage battery. A fuel cell system operation involves startup, fuel and air delivery control as a function of load, and removal of heat and by products of the reaction. The fuel cell, in other words, is an electrochemical engine. While electrochemistry describes the principle of operation of a fuel cell, the engineering challenge of balancing the many variables over a wide variety of operating conditions remains. The fuel cell system consists of a complex group of support systems that must operate in balance for efficient performance.

Different types of fuel cells are conveniently classified by the type of electrolyte they use. Electrolytes that are presently being considered include the proton exchange membrane (a solid polymer material), phosphoric acid (a liquid), alkaline (a liquid), molten carbonate (a liquid) and solid oxide (a ceramic). The choice of electrolyte directly affects a fuel cell's operating characteristics; for example, phosphoric acid is a poor ion conductor at room temperature. As a result the phosphoric acid fuel cell must be heated to 150 to 200^{o}C before it can be used. Today many researchers believe that the proton exchange membrane (PEM) provides the best characteristics for transportation applications.

The data and analysis presented in this paper is for a fuel cell system manufactured by Ballard Power Systems of Vancouver, Canada. The fuel cell system consists of: a 35 cell series connected stack; gas, water and thermal management subsystems; and controls and monitors all assembled in a single enclosure. The area of each cell was 232 cm^2 and the fuel cell stack itself had a maximum gross power output greater than 3000 Watts operating on hydrogen and air. The system was modified by the authors to be able to independently control air stoichiometry, air/hydrogen pressure and stack exit air temperature. Previous papers that have presented experimental data on similar Ballard fuel cells systems are references[1] and [2]

The paper is organized into sections in the following order; Fuel Cell Operating Principle, Experimental Apparatus, Experimental Results, Results Analysis and Conclusions. The section on fuel cell operating principle is intended to give a brief overview of how a fuel cell works and its operating characteristics. The experimental apparatus section briefly describes the fuel cell system used in the experiments and the associated instrumentation. The experimental results present a series of polarity plots (voltage - current relationship) under a variety of operating conditions. The results analysis section presents the results in terms of power density-efficiency plots implicitly demonstrating the

operating characteristics of the fuel cell system for electric vehicle applications.

FUEL CELL OPERATING PRINCIPLE

All energy-producing oxidation reactions are fundamentally the same and involve the release of chemical energy through the transfer of electrons. During combustion of hydrogen and oxygen there is an immediate transfer of electrons, heat is released and water is formed.

In a fuel cell the hydrogen and oxygen do not immediately come together but are separated by an electrolyte. First the electrons are separated from the hydrogen molecule by a catalyst (oxidation) creating a hydrogen ion (no electrons). The ion then passes through the electrolyte to the oxygen side. The electrons cannot pass through the electrolyte and are forced to take an external electrical circuit which leads to the oxygen side. The electrons can provide useful work as they pass through the external circuit. When the electrons reach the oxygen side they combine with the hydrogen ion and oxygen creating water. By forcing the electrons to take an external path, a low temperature direct energy conversion is achieved as shown in Figure 1.

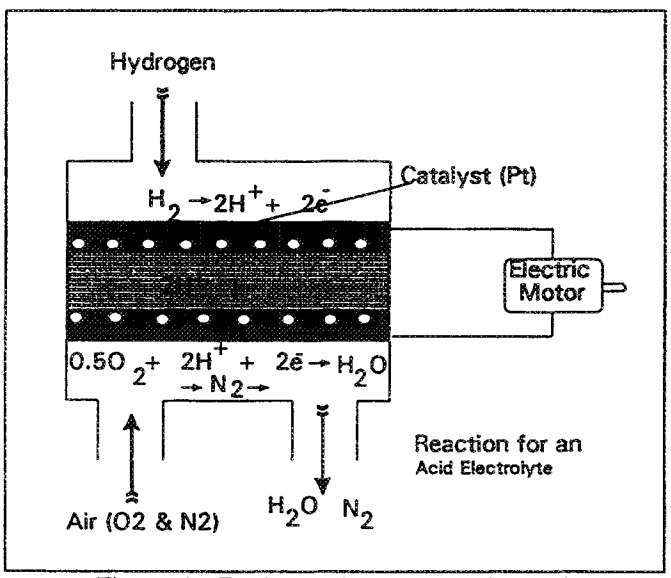

Figure 1. Fuel Cell Operation Schematic

The theoretical efficiency for the conversion of chemical energy into electrical energy in a hydrogen-oxygen fuel cell depends on the free energy of formation for the reaction (Gibbs Function). The free energy of formation is equal to the difference of the heating value of the fuel and its entropy at the temperature and pressure of conversion. This is described in equation 1.

$$\Delta G = \Delta H - T \times \Delta S \qquad (1)$$

Where

ΔH *Free energy of Formation*

T *Absolute Temeperature*

ΔS *Entropy*

Typically theoretical chemical to electrical conversion efficiencies are in the range of 83% for higher heating value and 94% for the lower heating value of hydrogen. Efficiencies of practical fuel cells using pure hydrogen and air range from 40% to 75% based on lower heating value of hydrogen.

Assuming a near perfect coulombic efficiency (all electrons are forced to take the external circuit) a theoretical operational voltage can be calculated. This voltage is calculated by considering Faraday's constant (26.8 Amp hours = 1 mole of electrons) and the energy value of the fuel. Table 1, provides the hydrogen/oxygen-water reaction enthalpy (heating value), the free energy of formation[3] and the resultant theoretical cell voltages.

Table 1 Hydrogen Thermodynamic Properties

Heating Value	ΔH Enthalpy of Formation kJ/Mole	Gibbs Function ΔG=ΔH-TΔS kJ/Mole At 25°C, 1 bar	Voltage Based on Enthalpy	Cell Voltage Based on Gibbs
Higher	-285.9	-237.2	1.48	1.23
Lower	-241.8	-228.6	1.25	1.18

Like a storage battery, when the fuel cell is under electrical load the voltage falls with maximum power generally being produced between 0.5 and 0.6 volts per cell. The voltage drop as a function of current is due to internal resistance (electronic and ionic), electrode kinetics (particularly on the air electrode), reactant gas flow limitations and product water flooding of reaction sites. To make a useful voltage, multiple cells are connected in electrical series, referred to as a stack as shown in Figure 2. Manifolds deliver reactant gases to the reaction sites. The fuel cell stack and all necessary auxiliaries are referred to as a fuel cell system.

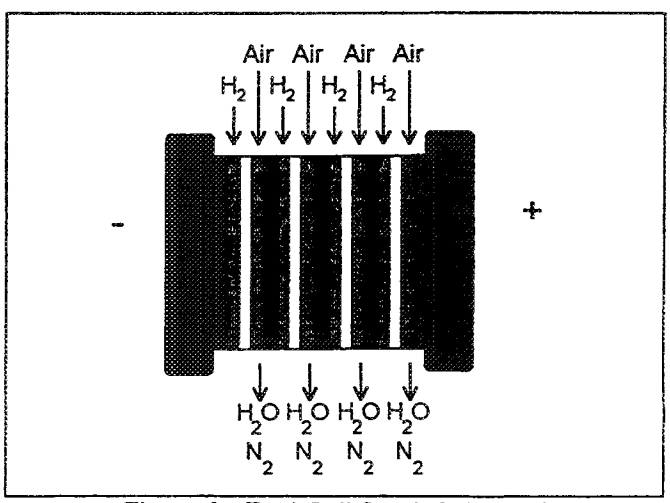

Figure 2. Fuel Cell Stack Schematic

The fuel cell stack design must allow for heat exchange and humidification of incoming reactant gases, thermal management, product water management, exhaust gases, and electrical management.

FUEL CELL SYSTEM DESCRIPTION - Given below are some of the specifications for the fuel cell power system which among others includes a 35 cell stack with a humidification section, temperature management, reaction product management and electrical control.

Table 2 Fuel Cell System Specifications.

Electrolyte	Nafion-117
# of Active Cells	35
Active Area/cell	232 cm^2
Total active area	8120 cm^2
Active Cell Thickness	0.5 cm
# of Cooling Cells	19
Active Plate Thickness	0.5 cm
# of Humidification Cells	14
System dimensions LxWxH	104 x 80 x 37 cm
System volume	307.8 liters
Stack dimensions LxWxH	38 x 21 x 21cm*
Stack volume	16.76 liters
Weight of the stack	43 kg
Weight of the system	50 kg
Support System Power **	350 Watts

*Includes active stack with humidification section and cooling cells
**water pump, hydrogen recirculation pump, fans, solenoid valve control and monitoring system

DATA ACQUISITION

One of the important tasks in the experiments conducted was to monitor and control the operating conditions of the fuel cell. The data acquisition and control system used signal conditioning modules which were capable of either data acquisition or control based on commands received from an IBM compatible personal computer. The modules communicated with the computer through an RS-232 communications port. Each module was isolated to 1500 volts and includes a filter to reduce noise. The control system involved both digital and analog input and output.

The load for the fuel cell was provided by resistive heater coils. The resistance provided to the fuel cell was controlled by a pulse width modulator (PWM). The PWM in turn was controlled by the analog output of the control system. The resistance could be controlled to provide a constant power or constant current load.

The variables measured by the control system included, stack current and voltage, support system current, load current, process air exit temperature, hydrogen inlet pressure, air inlet and outlet pressure. The digital signals monitored included the status of the load relay, hydrogen vent, oxidant vent and the water drain.

On the control side the load applied to the fuel cell was controlled by an analog output module. The digital output controlled the heat exchanger operation in order to maintain the temperature of the fuel cell at the required levels.

In order to maintain the stoichiometry of the air provided for the reaction a needle valve provided on the fuel cell was controlled. The flow rate was monitored by a flow meter installed in the air delivery line. Pressure control was established by using single stage pressure regulators.

Hydrogen for the fuel cell stack was provided from industrial hydrogen cylinders. The air system included a two stage compressor along with a chiller dryer and a system of air filters.

EXPERIMENTAL RESULTS

The experiment was organized into exploring the effects of three independent variables on performance: air stoichiometry, air pressure and exit air temperature. Air stoichiometry is the ratio of the amount of air provided to the fuel cell to that which is necessary to react with the hydrogen fuel. Other words used to describe this ratio include Lambda and excess air factor. In a typical internal combustion engine the value is very close to 1. Due to the operating nature of a fuel cell the stoichiometry of the air must be greater than one (typically 1.5 to 4). A lower value of stoichiometry reduces performance due to the lack of oxygen at the reaction sites. A high value of stoichiometry results in poor humidity control and excess compression energy.

The following test matrix illustrates the 12 different operating conditions over which the fuel cell system was characterized. The stoichiometric accuracy was held between +/- 0.1, the pressure accuracy was held between +/- 0.05 bar and the temperature accuracy between +/- 1.5°C. Under each operating condition the stack output current was varied between a minimum and maximum amperage at 10 amp intervals. The minimum current condition (20 amps) was limited by the support system power requirements and a small load on the electric load bank . The maximum current condition was limited by a minimum stack voltage of 19 (0.54 volts/cell). The minimum stack voltage was a limit set by Ballard power systems and was within a safe operating range for continuos operation of the system.

Table 3 Test Matrix For Fuel Cell Testing

Stoichiometry	Hydrogen and Air Pressure in Bar	Stack Exit Air Temperature °C
1.5	2	50, 60, 70
	3	50, 60, 70
2.0	2	50, 60, 70
	3	50, 60, 70

The results of this test matrix are organized into two polarity plots (Stoich.=1.5 and Stoich.=2.0), and an individual cell voltage characterization

POLARITY PLOTS - The polarity data resulting from the Table 2 test matrix is presented in Figures 3 and 4. These plots include the measured full stack data (volts and amps) and normalized data (volts/cell and milli amps/cm^2 of active area) The normalized data represents an average for the stack; actual individual cell data is presented in the following sub section.

Figure 3 presents the results for the six cases for which the stoichiometry was equal to 1.5. Figure 4 presents the

same results with the stoichometry equal to 2.0. The current range over which the two plots are described is the normal operating range of the fuel cell system. (Open circuit voltage, although not shown, was found to be approximately 1 volt per cell.).

Both, Figures 3 and 4, indicate a near linear relationship between voltage and current. The higher stoichiometry shown in Figure 4 results in a higher voltage at any given current compared to Figure 3. The difference in voltaic performance between the two stoich. rates is most pronounced at the high current levels. With a Stoich of 1.5 the fuel cell system could only deliver 130 amps before the low voltage limit was reached. In comparison, at a stoich rate of 2.0 the fuel cell could deliver approximately 160 amps. At a reference performance condition of 100 amps (normal operating condition) the average voltage increase with increase in stoich rate from 1.5 to 2 was 1.35 volts or 6.0 %. At lower current rates the percentage difference is smaller than at the higher rates. This seemingly small increase in voltage at a given current has the two-fold effect of increasing power and operating efficiency. In the following section; 'Results Analysis', it will be shown that even a relatively small increase in voltage has a significant impact on performance for an electric vehicle.

As a function of pressure, voltaic performance also increased. Once again utilizing a reference performance condition of 100 amps the typical voltage increase going from 2 to 3 bar was between 0.5 and 1.2 volts (2 to 5%). Voltaic performance also increased as a function of temperature . Once again utilizing a reference performance condition of 100 amps the typical voltage increase observed for an increase in temperature from 50 to 60 °C was 0.5 to 1.0 volts (2 to 4%), for an increase from 60 to 70 °C the corresponding voltage increase was 0.3 to 0.7 volts (1 to 3 %). The benefit of going from 60 to 70°C was less than going from 50 to 60°C There will be an optimum operating temperature for the fuel cell beyond which the voltaic performance will decline. The experimental data indicates that this value is probably greater than 70°C.

For both the pressure and temperature changes the percentage change in voltaic performance is greater at high current rates. Once again this seemingly small increase in voltage at a given current has the two-fold effect of increasing power and operating efficiency. Thus a relatively small increase in voltage has a significant impact in performance for an electric vehicle.

INDIVIDUAL CELL PERFORMANCE - The voltage performance of individual cells was measured at a exit air temperature of 60°C and a pressure of 3 bar. Five different stack current rates were used (20, 40, 70, 100, 130 amps) and the respective cell voltages are presented in Figure 5. The measurements were manually made utilizing a digital volt meter and pointed probes directly on to the active cell plate edge.

Figure 5 shows that there is a difference in voltaic performance for each cell at a given current rate. The differences in performance are consistent over the operating current range, a cell that shows a lower voltage at a low current density continues to have a lower voltage at higher current densities. The lower voltage could be the result of the difference in the electrode membrane assembly, distribution of reactant gases, internal cell resistance or a persistent flooding effectively reducing the available reactive area.

Although not shown, individual cell performance has been measured several times over the 6 months of preparation to conduct the experiments described in this paper. Consistently cells 6 and 25 have had a lower voltaic performance than the other cells (0.05 volts lower than average for 100 amps). As a result the authors feel that difference is inherent to the particular cells and not a transient phenomena due to a flooding condition or other temporary phenomena. It is interesting to note that cells 7, 24 and 26 perform above average, these high performance cells are adjacent to the lowest performing cell and may indicate that the problem is one of flow distribution.

The following Table 4 summarizes the results of the individual cell measurements. Although Figure 5 shows a consistent pattern of cells 6 and 25 having lower than average voltage the overall stack performance is very good. The maximum voltage spread is the result of cells 6 and 25 while the standard deviation is very small due to the generally consistent performance of the stack.

Table 4 Individual Cell Voltage Characteristics

Stack Current	20	40	70	100	130
Stack Voltage	30.25	28.4	26.5	24.4	22.4
Current Density mA/cm^2	86	172	302	431	560
Average Cell Voltage	0.864	0.812	0.758	0.698	0.640
Maximum Voltage Spread	0.03	0.042	0.063	0.086	0.115
Cell Voltage Standard Deviation Volts	.006	.008	.0115	.017	.025

SUPPORT SYSTEMS ELECTRICAL LOAD - The fuel cell system has support components that are electrically operated and controlled. Support system power is drawn from the fuel cell stack through a voltage regulated power supply (constant 26 volt output). The support components include a combined cooling and reactant gas humidification system that recovers product water from the stack exit air, a hydrogen recirculation system, and a control system that monitors and controls the start up, operation and shut down of the fuel cell system.

The combined cooling and humidification system utilizes a circulation water pump that provides water to cooling plates followed by the reactant gas humidification section. Based on stack exit air temperature the water leaving the humidification section is routed through a water to air heat exchanger. The hydrogen recirculation system maintains a constant recirculation rate through the stack and a liquid water knock out drum. This circulation combined with periodic purges prevents flooding conditions and build up of inert gas on the hydrogen side of the fuel cell stack.

Table 5. gives the support system load demand during operation of the fuel cell. The support system power requirement does not include air compression which is independent of the fuel cell stack output. As a result the support system power (a parasitic loss) varies in percentage of stack power from 100% (idle condition) to 10% (full power condition. The difference in support system power (250 to 400 Watts) results from the cooling of the circulating water. When the water is circulated through the water to air heat exchanger the additional power is drawn by ventilation fans.

Table 5 Support Systems Loads

Component	Amps
Water Pump	3-4
Hydrogen Circulation pump	1
Ventilation Fans	2
Controller, batteries and solenoids	3-6
Total Support System	10 to 15 (250 to 400 Watts

RESULTS ANALYSIS

The previous sections described fuel cell polarity plots, which is a standard method to describe fuel cell performance. However, the interests of an automotive engineer in applying a fuel cell to an electric vehicle is better described in terms of power and efficiency. The specific power available determines the size of the fuel cell system and to some extent its cost. The conversion efficiency affects the sizing of the fuel storage, resultant range and refueling times.

To accommodate this need for a power and efficiency relationship the polarity data can be reinterpreted. The specific power of the fuel cell is simply the ratio of the product of the stack voltage and the stack current to the total available active electrolyte area.

$$\text{Specific Power} = \frac{V \times I}{\text{Total Active Area}} \times 1000 \quad \left(\frac{\text{mWatts}}{\text{cm}^2}\right) \quad (2)$$

Where

V Stack Voltage

I Stack Current

To calculate the fuel cell stack gross conversion efficiency it is assumed that the system is operating at a perfect coulombic efficiency (all available electrons from the hydrogen fuel were forced to take the external circuit providing useful work). This means that all inefficiencies are manifested in a voltaic loss. Equation 3 presents the method used to calculate fuel cell stack conversion efficiency. This approach to calculating efficiency is generally considered valid for the proton exchange membrane fuel cell, however measurements will be made in the future using this same fuel cell system to quantify this assumption. See the earlier section, 'Fuel Cell Operating Principle', for further details. Note that no allowance is made for the support system power requirements or air compression. As a result the net efficiency of conversion (ratio of delivered electrical energy to chemical energy) is less than the fuel cell stack conversion efficiency

$$\text{Fuel Cell Stack Conversion Eff.} = \frac{V}{1.25 \times 35} \times 100\ \% \quad (3)$$

Where

V *Stack Voltage*

1.25 *Theoretical Cell Voltage Based on Enthalpy of Formation (Lower)*

35 *Number of Cells in Stack*

Utilizing equations 2 and 3 the data presented in Figures 4 and 5 was recalculated and presented in Figures 6 through 9. Figures 6 through 9 present the fuel cell stack specific power as a function of fuel cell stack conversion efficiency based on the lower heating value of hydrogen. In these figures a higher electrode power density translates to a smaller electrode area to achieve a given power level. A high conversion efficiency translates to a smaller fuel storage and refueling time for a given vehicle range and performance. A second order affect is that a higher efficiency translates to smaller heat generation within the fuel cell system thus a smaller heat exchanger system and other support components.

Figures 6 through 9 are organized as a function of stoichometry and operating pressure. Figures 6 and 7 present specific power data for a stoich of 1.5 and pressures of 2 and 3 bar respectively. Each figure shows the results for the three different temperatures in the test matrix (50 60 and 70 °C).

Consider Figure 6, the specific power-efficiency curves indicate a trade-off between power and efficiency. The higher the specific power density, the lower is the conversion efficiency. The relationship between specific power and efficiency appears linear for high conversion efficiencies, 70% to approximately 55%. At this point the power increase for the drop in efficiency becomes less and the curve starts to flatten. Although the curve does not distinctly show a specific power peak the data indicates that this peak is somewhere around 45% energy conversion efficiency, this corresponds to an average cell voltage of approximately 0.55 (just slightly greater than one half the open circuit voltage). Increasing the current beyond the peak power point results in a further decline in specific power and conversion efficiency. At no time would it be advantageous to operate the fuel cell system beyond the peak power point.

The following analysis utilizes three different specific power conditions to illustrate the influence of stoichometry, pressure and temperature. The three specific power conditions selected are 125 mW/cm^2, 275 mW/cm^2, and 325 mW/cm^2. The low power condition (125) relates to a possible cruise condition for the electric vehicle, the high power condition (275) relates to acceleration or hill climbing. The highest specific power 325 was not attainable by the system at low stoichometry and pressure and is used to illustrate the enhanced capability by changing operating conditions. Table 6 relates the energy conversion efficiency to the three selected specific power conditions.

First comparing the affect of stoichometry, the efficiencies of operation in Table 6 immediately shows that at low power conditions stoichiometry has little influence on efficiency of operation resulting only in 1 to 2 percentage points increase. At the higher power condition the spread increases to 4 to 5 percentage points or in other words a 10% change in stack fuel consumption for the same power level. At the highest power condition the increase in stoichiometry is necessary for the stack to reach the 325 mW/cm^2 specific power level The low stoichiometry simply cannot reach the high level having peaked at approximately 290 mW/cm^2. Increased stoichiometry is most beneficial at high power conditions.

Table 6 Fuel Cell Stack Conversion Efficiency at Three Specific Power Points

Operating Condition	Speci. Power 125 mW/cm^2	Speci. Power 275 mW/cm^2	Speci. Power 325 mW/cm^2
S=1.5, T=60C, P =2 Bar	64%	51%	not possible
S=1.5, T=60C, P =3 Bar	64%	54%	46%
S=2.0, T=60C, P =2 Bar	65%	56%	50%
S=2.0, T=60C, P =3 Bar	66%	58%	53%

Comparing the influence of an air pressure change from 2 bar to 3 bar there is almost no difference for the low power case. Under high power conditions the change in pressure increases the efficiency by 2 to 3 percentage points or a difference of 6% in stack fuel consumption for the same power level. For the highest power condition a pressure change from 2 to 3 bar allows the lower stoichometry of 1.5 to reach high power of 325 mW/cm^2, however the lower stoichiometry has a energy conversion efficiency 7% points lower or a stack fuel consumption of 15% higher. Like stoichiometry the benefit of pressure is most pronounced at high power conditions. Both increased pressure and stoichiometry increase the compression power needed to operate under these conditions. As a result, choosing the stoichiometry and operating pressure is not a simple straight forward procedure. The affect of air compression power will be examined in a following section.

Table 7 compares the influence of temperature on performance for a stoichiometry of 2, the two different pressure cases are presented for comparison. Once again at a low specific power there is little difference in efficiency. At the high power level the efficiency spread resulting from an increase temperature is between 3 and 5% points. At the highest power level the low temperature low pressure case can not achieve 325 mW/cm^2. By increasing the temperature to 70°C the highest power condition was possible at a conversion efficiency of 51%. The effect of temperature rise on the 3 bar pressure case was to increase efficiency by 3 % points, or a difference in stack fuel consumption of 6%. There will be an optimum operating temperature for the fuel cell beyond which the conversion efficiency for a given specific power will decline. The experimental data indicates that this value is probably greater than 70°C. The high operating temperature reduces the sizing of the fuel cell cooling system by a. Further there is no additional support energy required to maintain the fuel operating temperature at a high value.

Table 7 Fuel Cell Stack Conversion Efficiency at Three Specific Power Points

Operating Condition	Speci. Power 125 mW/cm^2	Speci. Power 275 mW/cm^2	Speci. Power 325 mW/cm^2
S=2.0, T=50C, P =2 Bar	64%	52%	not possible
S=2.0, T=70C, P =2 Bar	65%	57%	51%
S=2.0, T=50C, P =3 Bar	66%	56%	52%
S=2.0, T=70C, P =3 Bar	67%	59%	55%

This analysis also indicates the clear advantage that a fuel cell has at part load condition. Unlike an internal combustion engine the energy conversion efficiency increases substantially as the load is reduced (typically 15 percentage points or a fuel reduction of 25% for a kWh produced). Not evident in this analysis is that highly dynamic operation does not degrade the efficiency. Operating on hydrogen the fuel cell responds instantaneously to the new operating load with no loss in efficiency for the change in power condition[4]. A difficult that does arise under dynamic conditions is the need to control the air flow at prescribed stoichiometric rates.

This combination of high part load efficiency and no degradation due to dynamic operation gives the fuel cell a clear advantage over the internal combustion engine. This advantage is particularly important for a city driving cycle.

AIR COMPRESSION ENERGY - The support system for a fuel cell power plant include controls, cooling fans, recirculation pumps (water and hydrogen) and compressed process air. The difference between fuel cell stack power and fuel cell system power is due to the parasitic losses associated with the support system components. Of these components and the energy required to operate them the compressed air energy requirement is by far the largest.

Pressurization of air improves the performance of the fuel cell when considered as an individual entity. However, the energy for compression on an electric vehicle must be supplied by the fuel cell system, and thus net power output is less than the gross stack performance. The air compression process can be adiabatic or isothermal and part of the compression energy may be recovered from the exiting air by an expander such as a turbine. To determine the influence the energy of compression would have on the fuel cell performance the following analysis assumes that the compression is performed by an ideal adiabatic compressor with no energy recovery upon expansion. The affect of the air compressor can be related to a simple loss in net cell voltage as a function of pressure ratio and stoichiometry. A full derivation may be found in reference[5] a brief explanation is provide in the following paragraph.

Air compression power is a function of inlet to outlet pressure ratio and the quantity of air compressed. The relationship of compressor power to quantity of air compressed is linear. For a constant stoichiometric the quantity of air needed is directly related to the current being produced. Double the current, double the air is needed to maintain the stoichometry, double the compressor power is needed to maintain the flow. Consider an ideal compressor in

series with the electrical load. When the fuel cell current is increased the compressor power must increase in direct proportion. Because the current has gone up the voltage drop across the compressor remains the same. The voltage available to the electrical load (net voltage) is simply the cell voltage minus the effective compressor voltage that is a constant for a give stoichiometry and pressure ratio. Thus the effect of air compression can be simply presented effectively as a reduction in voltage. Utilizing equation 3, this effective compressor voltage loss can be used to determine the impact air compression has on efficiency. The following equation to calculate effective compressor voltage was first derived in reference[6]

$$V_c = \frac{1.287}{3600} \times \#\text{ of Stoich.} \times C_p T_1 \left(\frac{P_2}{P_1}^{\frac{k-1}{k}} - 1 \right) \quad (4)$$

Where

V_c *Effective Adiabatic Compressor Voltage loss per Cell*
C_p *Specific Heat (Air 1.004 J/(g °K))*
T_1 *Compressor Inlet Air Temperature °K*
P_1 *Compressor Inlet Air Pressure*
P_2 *Compressor Outlet Air Pressure*
k *Specific Heat Ratio (Air 1.4)*

Utilizing equation 4 the effective compressor voltage loss for the 35 cell stack data presented in this paper is tabulated in Table 8. The voltage loss has been interpreted as an efficiency reduction and is presented in brackets.

Table 8 Effective Adiabatic Compression Voltage Loss and Resultant Efficiency Loss

Stoich	Press = 2 Bar	Press = 3 Bar
1.5	1.23 volts (-2.8%)	2.07 volts (-4.7%)
2	1.64 volts (-3.7%)	2.77 volts (-6.3%)

Table 8 indicates that the affect of the energy of air compression is to reduce operating efficiency by 2.8 to 6.3 percentage points. Considering that air must be forced through the fuel cell stack the 2 Bar case will be considered as a base lines. Increasing the pressure from 2 to 3 bar increase the effective degradation in efficiency by 1.9 to 2.6 percentage points.

In the previous subsection the influence of a pressure change from 2 to 3 bar on efficiency at low specific power conditions was found to be 1 percentage point or less, thus the net effect of compression would be negative. At high power conditions the affect of pressure change from 2 to 3 bar is to increase conversion efficiency by 3 percentage points. This gain is almost entirely nullified by the effective compressor efficiency loss.

Utilizing the data for a stoichiometry of 2 at 60°C the performance of pressure equal to 2 bar and 3 bar is compared in Figure 10. The fuel cell stack specific power for the 3 bar case is higher then the 2 bar case. However when the effective compressor voltage loss is considered (Table 8 values) the performance of the 2 bar case exceeds the 3 bar case. The 3 bar case has a higher peak power value but it is notably lower efficiency.

Air compression decreases the conversion efficiency of fuel cell system. It also impacts the peak specific power available. A high stack performance from increasing the operating pressure may not be enough to over come the additional power requirement of the compressor.

CONCLUSIONS

The 3 kW fuel cell system described in this paper is an impressive performer with approximately 40 hours of operation in preparing and obtaining the presented data. Measured energy conversion efficiencies while operating on hydrogen and air ranged between 45% and 70%. Under part load conditions (1 to 2 kW the efficiency typically ranged between 55 and 65% , peak power output (3 kW) typically occurring at 45%. The trade off between power and efficiency will influence the sizing of the fuel cell system. For a given vehicle application a larger more expensive fuel cell will operate at a lower average power and thus have a better fuel economy.

The result of increasing the fuel cell operating pressure and stoichiometry is to increase its performance. The influence of these two parameters was found to be dependent on the fuel cell electrical load. At low load conditions increasing stoichiometry or pressure had little influence. At high load conditions increasing the stoichiometry from 1.5 to 2 improved performance by as much as 7 percentage points. This would effectively reduce stack fuel consumption by 15% for the same amount of energy conversion. Increasing the operating pressure from 2 to 3 bar would improve stack performance as much as 3 percentage points or an effect fuel consumption drop of 7%.

The benefits of increased stoichiometry and pressure must be balanced against the power needed to compress the additional air to a higher pressure. A brief analysis of the calculated adiabatic compression power with no pressure recovery was presented. The analysis found that based on the experimental data there was no net advantage in increasing the operational air pressure from 2 to 3 bar. This calculated result indicates the trade off between stoichometry, pressure and the energy of compression is not a simple one. Other support components that must be powered by the fuel cell include controls, a water pump and a hydrogen recirculation pump. These components required a near constant 250 to 350 Watts (10% of maximum fuel cell stack power) and were independent of the fuel cell system power output. Both pumps were operated at constant rates and sized for maximum operating conditions. In an automotive design they will be variable and thus reduce the percentage power requirements of the pumps significantly.

The affect of increasing the operational temperature (stack exit air temperature) from 50 to 60 to 70 °C was an improvement in performance. There is an optimum operating temperature for the fuel cell stack beyond which the performance will decline. The experimental data indicates that this value is probably greater than 70°C. High operating

temperature reduces the sizing of the fuel cell cooling system and is considered an advantage.

Individual cell voltaic performance was measured and found to have slight variations between cells. Two cells in particular had lower voltages (0.1 volts below average at a current of 130 amps). Adjacent to these cells were cell performing above average, indicating possible reactant gas flow distribution problem. Unlike a storage battery the lower voltaic performance is not a serious problem.

The fuel cell power system is a strong candidate to meet the needs of California's ZEV mandates. Utilizing on-board hydrogen the only byproduct of operation is water. The high conversion efficiency of a fuel cell overcomes many of the storage and cost problems associated with hydrogen. The promise of fuel cell technology is a ZEV with the performance, range and rapid refueling capability of conventional vehicles.

ACKNOWLEDGMENTS

The authors wish to thank Ballard Power Systems and California Department of Transportation (New Technologies Division) for the support they have provided in setting up the fuel cell laboratory at the Institute of Transportation Studies, Davis. We also wish to thank the University of California Transportation Center for financially supporting the Graduate Students involved in this project. Last but not the least we wish to thank Mr. Gonzalo Gomez and Mr. Manohar Prabhu for their assistance in setting up the data acquisition and control system and helping us in obtaining the experimental data.

REFERENCES

[1] Prater K. B., "Solid Polymer Fuel Cell Developments at Ballard", Procedings of the 2nd Grove Symposium, Editors A.J. Appleby and D.G. Lovering, 1991 p 189 to 201.

[2] Olivera C.T., A. Anantaraman and W.A. Adams, "Performance Evaluation of a H2/Air PEM-FC System under Variable Load", Precedings of the 1992 Fuel Cell Seminar, Tucson, Arizons, December 1992 p 451 to 454

[3] Masterton W.L., E.J Slowinski, "Chemical Principles", W.B. Saunders Co. Philadelphia PA, 1973.

[4] Dickinson B.E., T. Lalk, D. G. Hervey, "Characterization of a Fuel Cell/Battery Hybrid System for Electric Vehicle Applications", SAE Paper 931818, published in Special Publication 984, 1993.

[5] Swan D.H , A.J. Appleby, "Fuel Cells for Electric Vehicles, Knowledge Gaps and Development Priortities", Proceedings of The Urban Electric Vehicle, Stockholm Sweden, pp 457-468, May 1992.

[6] Swan D.H., O.A. Velev, I.J. Kakwan, A.C. Ferreria, S. Srinivasan, A.J. Appleby, "The Proton Exchange Membrane Fuel Cell - A Strong Candidate as A Power Source for Electric Vehicles", Hydrogen 91 Technical Proceedings, International Association for Hydrogen Energy, 1991.

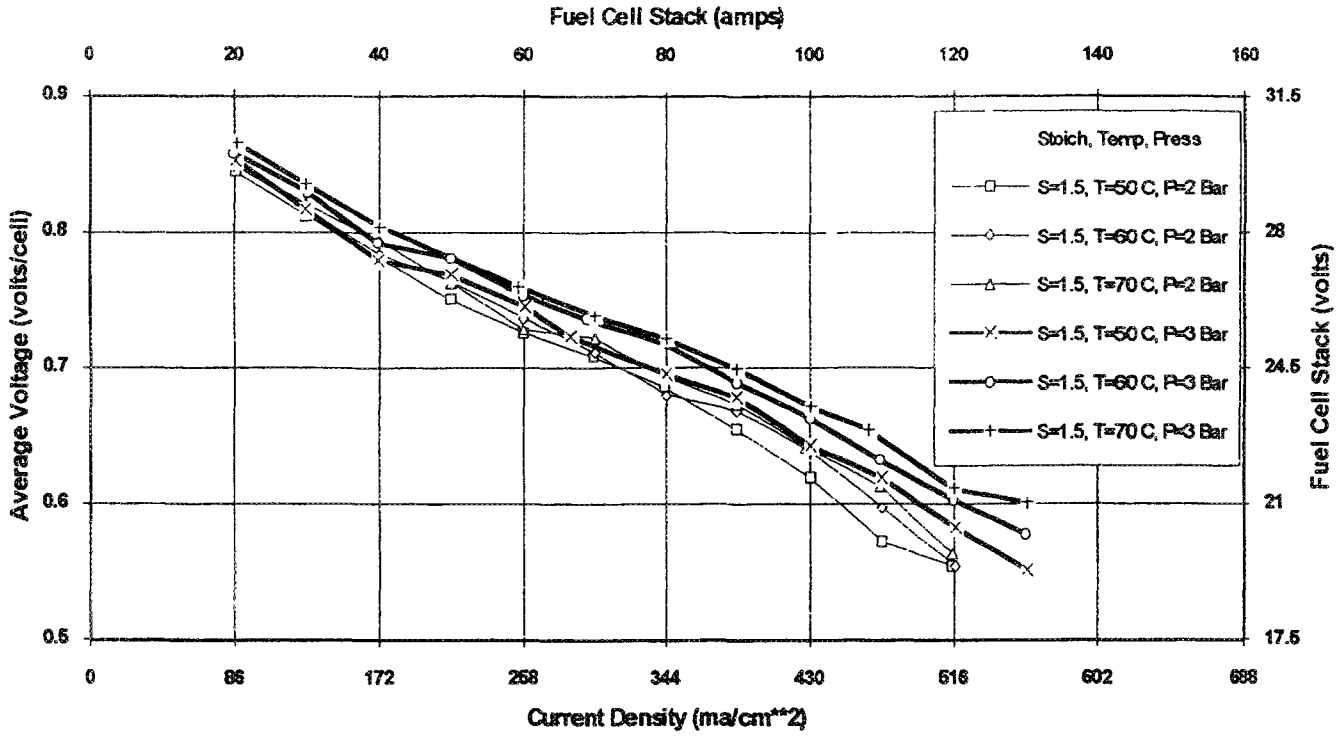

Figure 3. Fuel Cell Stack Polarity Plot for Stoichiometry of 1.5

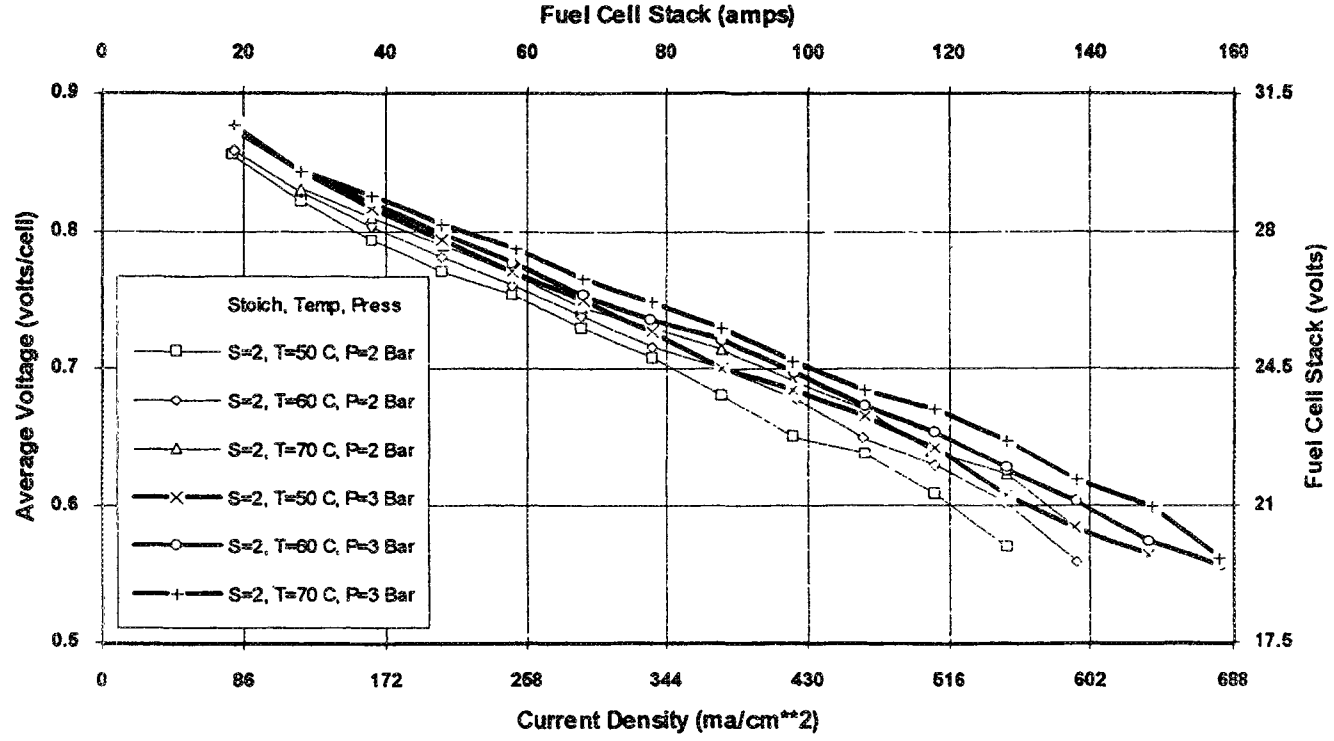

Figure 4. Fuel Cell Stack Polarity Plot for Stoichiometry of 2.0

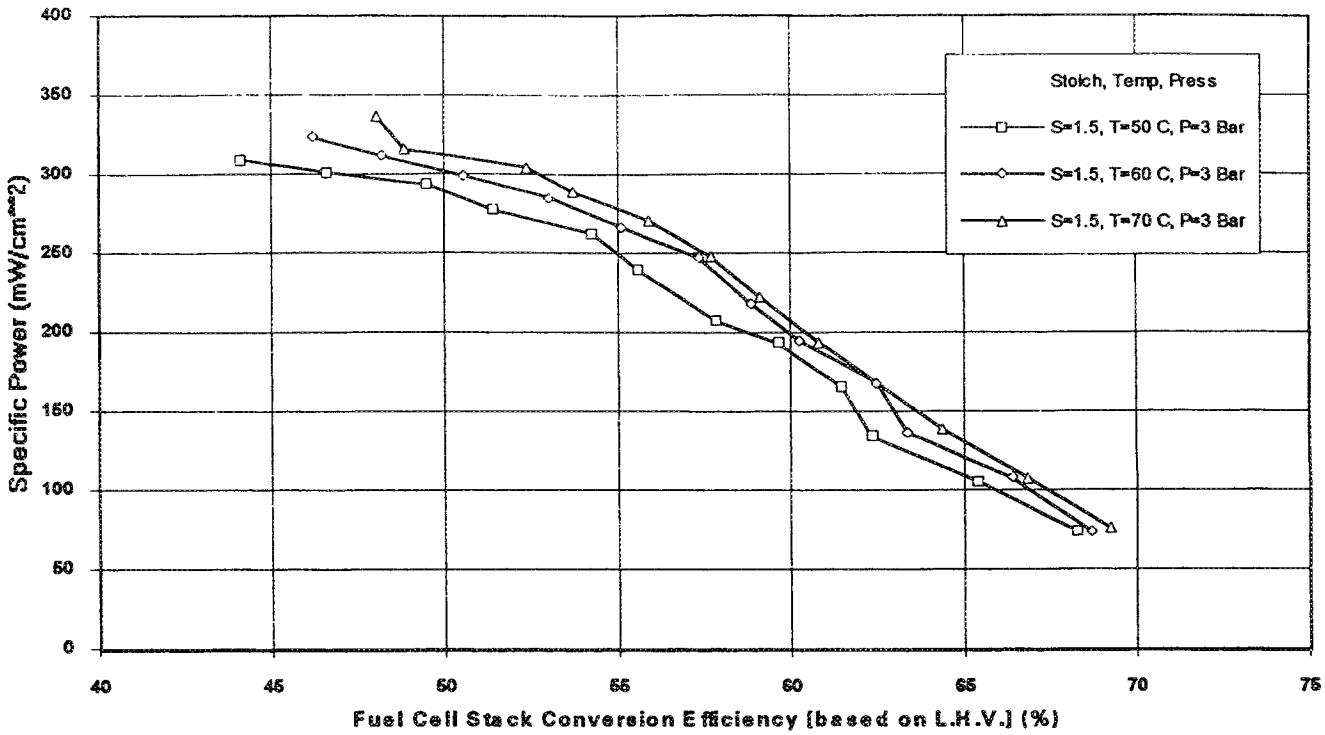

Figure 7. Specific Power as a Function of Temperature and Efficiency for Stoichiometry of 1.5, Pressure = 3 Bar

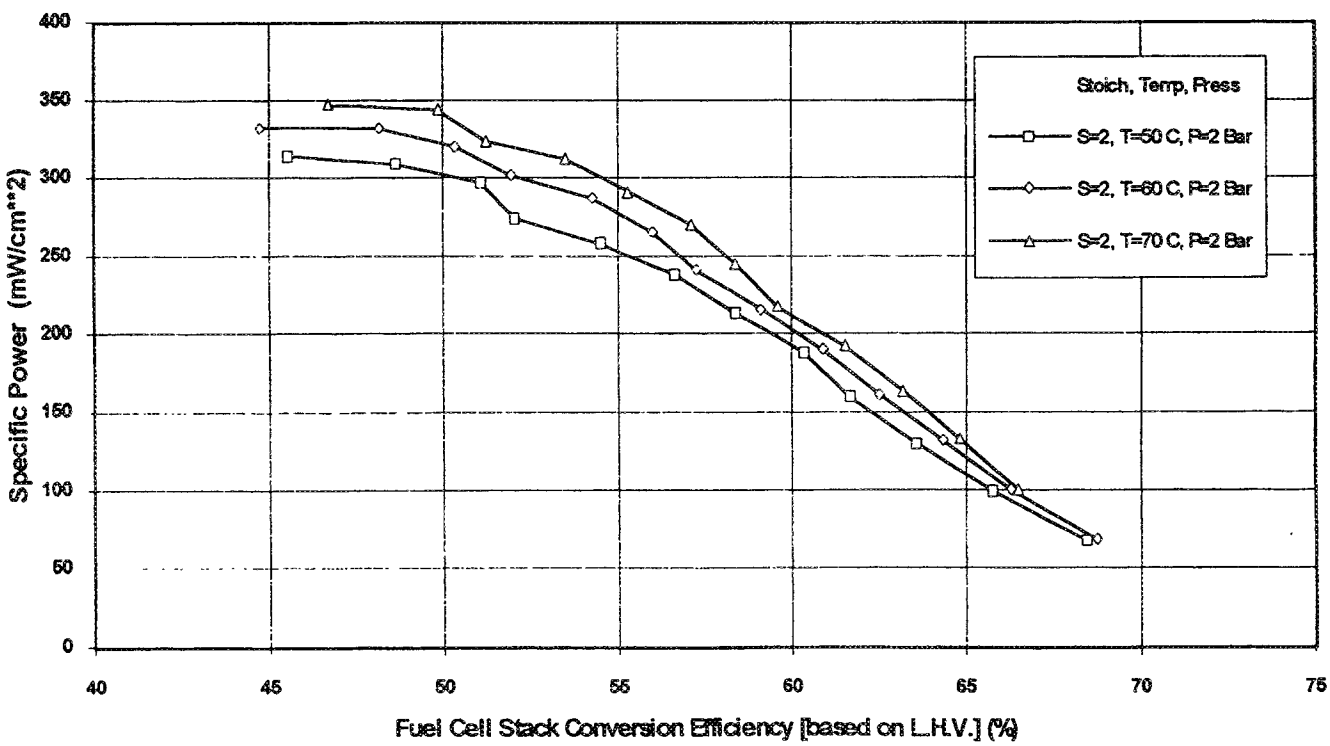

Figure 8. Specific Power as a Function of Temperature and Efficiency for Stoichiometry of 2.0, Pressure = 2 Bar

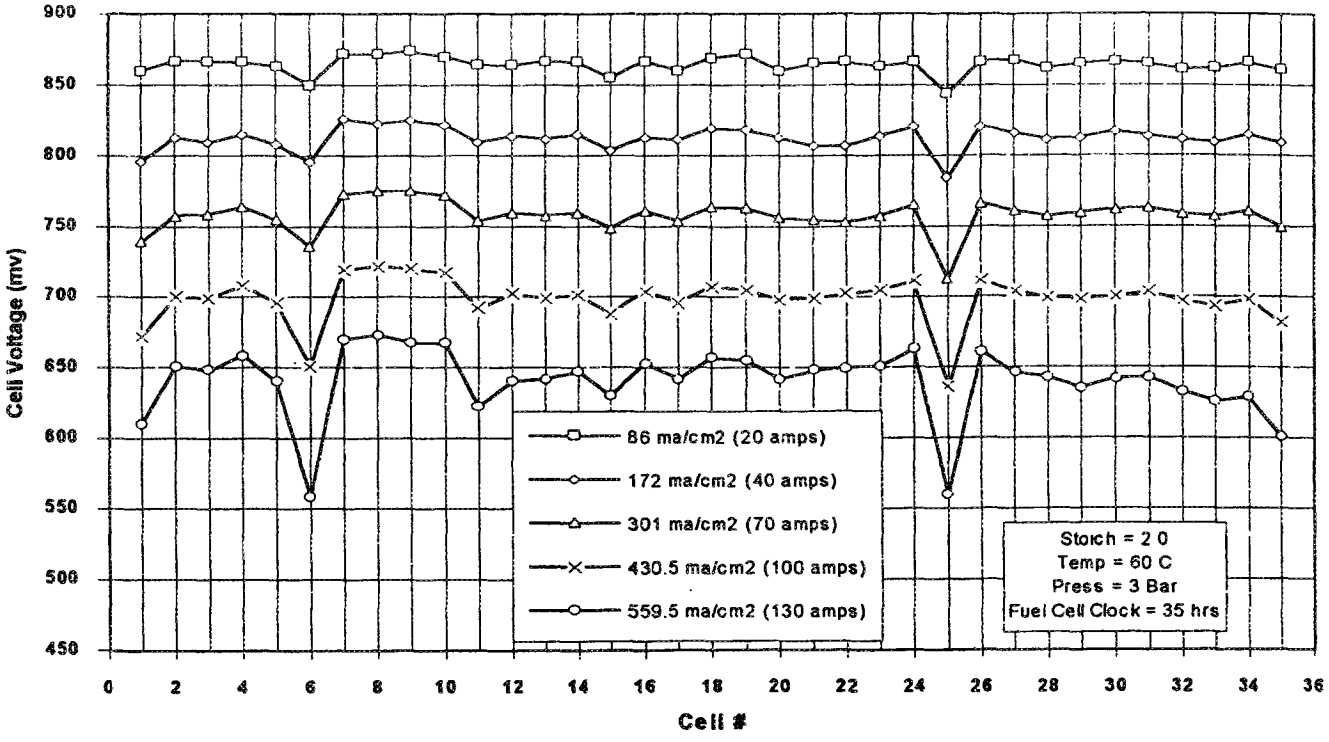

Figure 5. Individual Cell Voltages at Different Current Densities

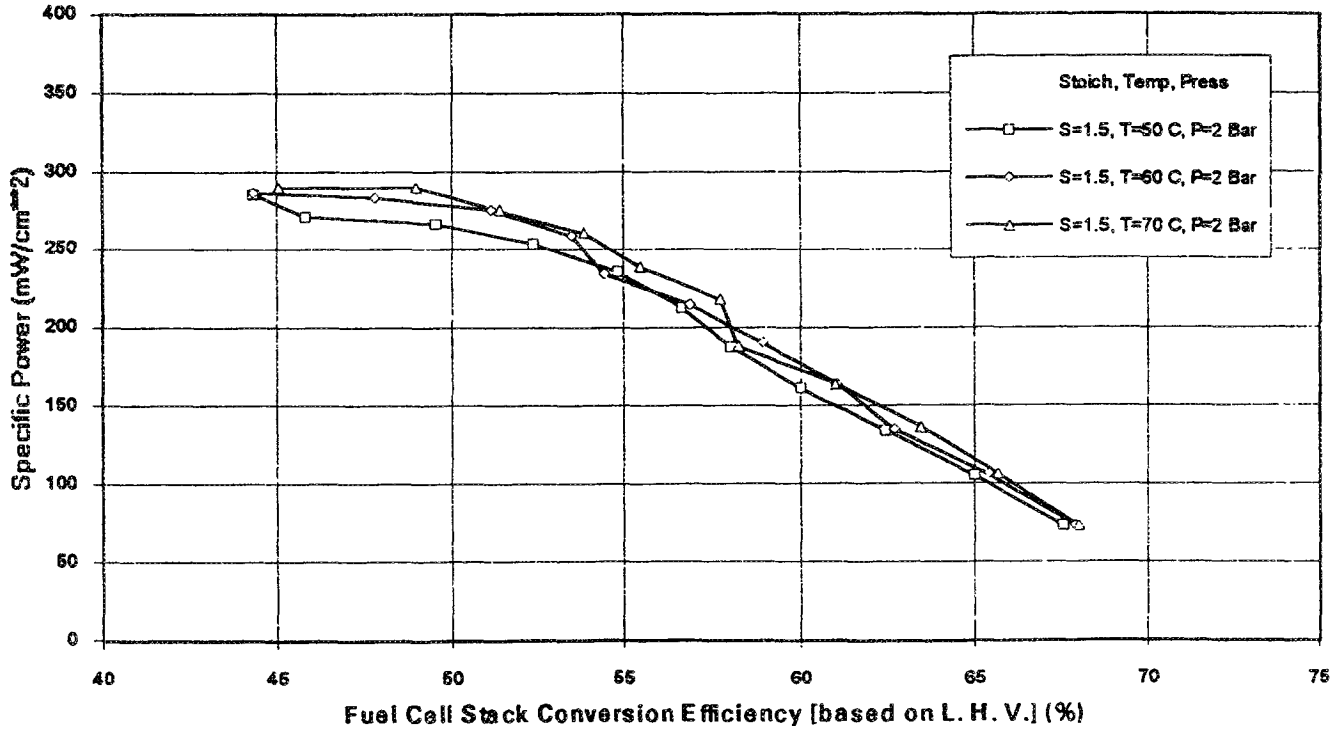

Figure 6. Specific Power as a Function of Temperature and Efficiency for Stoichiometry of 1.5, Pressure = 2 Bar

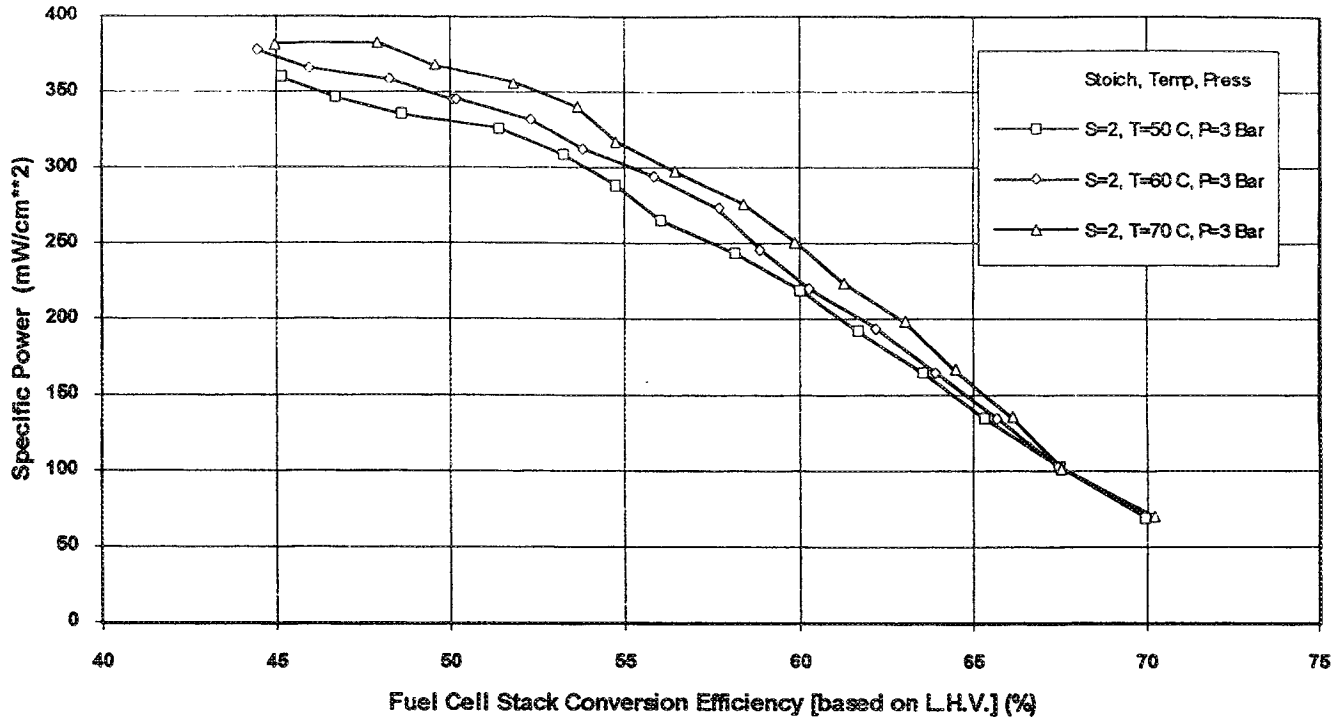

Figure 9. Specific Power as a Function of Temperature and Efficiency for Stoichiometry of 2.0, Pressure = 3 Bar

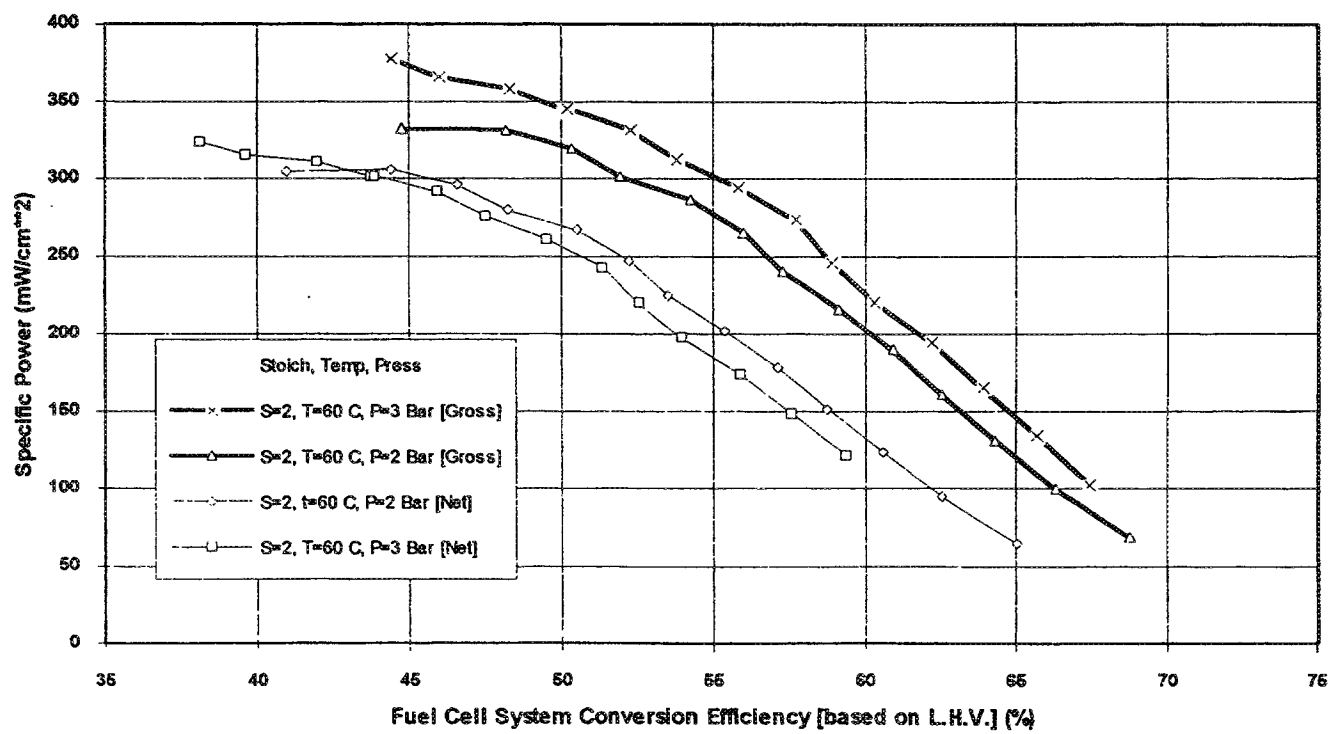

Figure 10. Comparison of Gross and Net Fuel Cell System Specific Power at Pressures of 2 and 3 Bar